

## Solvent-Stabilized Molecular Capsules

Alexander Shivanyuk, Jan C. Friese, Steve Döring, and Julius Rebek, Jr.\*

The Skaggs Institute for Chemical Biology and The Department of Chemistry, The Scripps Research Institute, MB-26, 10550 North Torrey Pines Road, La Jolla, California 92037

jrebek@scripps.edu

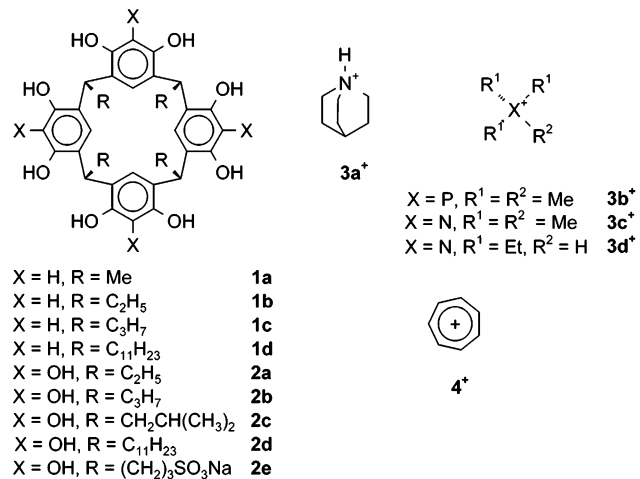
Received June 9, 2003

Pyrrogallolarenes **2** were prepared by acid-catalyzed condensation of pyrogallol with aldehydes. Compound **2a** crystallizes from a methanol solution of quinuclidine hydrochloride to give a dimeric molecular capsule surrounding one disordered quinuclidinium cation. The molecules of **2a** are connected by direct hydrogen bonds and by bridging methanol and water molecules. The chloride anion is positioned outside the capsule and is hydrogen bonded to the hydroxy groups of **2a**. The shortest distance between the cation and anion was found to be 6.7 Å. Crystallization of **2b** from aqueous acetonitrile resulted in a dimeric capsule linked by a polar belt of 16 hydrogen bonding water molecules. Four acetonitrile molecules occupy the cavity of this dimeric capsule and assume two binding sites that differ in hydrogen bonding and electronic environment. Compounds **2** also form hydrogen-bonded dimeric molecular capsules in alcohols and aqueous acetonitrile solutions. These assemblies readily encapsulate tetramethylammonium, tetramethylphosphonium, quinuclidinium, and tropylium cations to give complexes stable on the NMR time scale at 233 K.

## Introduction

Self-assembling molecular capsules are known to encapsulate a variety of neutral and charged guests in solution, in the solid state, and in the gas phase.<sup>1</sup> Capsules formed through cooperation of strong metal coordination bonds<sup>2</sup> are usually required for stability in highly polar solvents such as alcohols and water, but multiple intermolecular electrostatic interactions can also produce stable capsular assemblies in aqueous or alcohol solutions.<sup>3</sup> Hydrogen-bonded capsules<sup>4</sup> form in apolar solvents and are easily disassembled by the addition of small amounts of competitive solvents. Accordingly, many tactics have been deployed to stabilize them in such media. In some cases, polar, hydrogen-bonding solvent molecules can provide essential parts of multicomponent capsular assemblies. Specifically, water and 2-propanol molecules act as hydrogen-bonding links between hemispherical resorcinarene modules **1a,b,d** (Chart 1) in the

## CHART 1



\* Corresponding author. Phone: (858) 784-2250. Fax: (858) 784-2876

(1) For reviews see: (a) Hof, F.; Craig, S. L.; Nuckolls, C.; Rebek, J., Jr. *Angew. Chem., Int. Ed.* **2002**, *41*, 1488–1508. (b) Rudkevich, D. M.; Rebek, J., Jr. *Eur. J. Org. Chem.* **1999**, 1991–2005. (c) Conn, M. M.; Rebek, J., Jr. *Chem. Rev.* **1997**, *97*, 1647–1668. (d) MacGillivray, L. R.; Atwood, J. L. *Angew. Chem., Int. Ed.* **1999**, *38*, 1018–1033. (e) Rudkevich, D. M. *Bull. Chem. Soc. Jpn.* **2002**, *75*, 393–413.

(2) (a) Fujita, M.; Umemoto, K.; Yoshizawa, M.; Fujita, N.; Kusukawa, T.; Biradha, K. *Chem. Commun.* **2001**, 509–518. (b) Fox, O. D.; Dalley, N. K.; Harrison, R. G. *J. Am. Chem. Soc.* **1998**, *120*, 7111–7112.

(3) (a) Corbellini, F.; Fiammengo, R.; Timmerman, P.; Crego-Calama, M.; Versluis, K.; Heck, A. J. R.; Luyten, I.; Reinhoudt, D. N. *J. Am. Chem. Soc.* **2002**, *124*, 6569–6575. (b) Fiammengo, R.; Timmerman, P.; de Jong, F.; Reinhoudt, D. N. *Chem. Commun.* **2000**, 2313–2314. (c) Brewster, E. B.; Shuker, S. B. *J. Am. Chem. Soc.* **2002**, *124*, 7902–7903.

(4) (a) Rebek, J., Jr. *Chem. Commun.* **2000**, 637–643. (b) Rebek, J., Jr. *Acc. Chem. Res.* **1999**, *32*, 278–286.

solid state. With this help, both dimeric and hexameric capsules can be assembled.<sup>5</sup> Lipophilic resorcinarene **1d** assembles into a hexameric capsular complex in water-saturated chloroform or benzene.<sup>6</sup> In dry solvents only ill-defined aggregates are formed. Hydrogen bonding between cavitand tetrabenzimidazoles and water mol-

(5) (a) Murayama, K.; Aoki, K. *Chem. Commun.* **1998**, 607–608. (b) Rose, K. N.; Barbour, L. G.; Orr, G. W.; Atwood, J. L. *Chem. Commun.* **1998**, 407–408. (c) Mansikkamaki, H.; Nissinen, M.; Rissanen, K. *Chem. Commun.* **2002**, 1902–1903. (d) MacGillivray, L. R.; Atwood, J. L. *Nature* **1997**, *389*, 469–472.

(6) (a) Shivanyuk, A.; Rebek, J., Jr. *Proc. Natl. Acad. U.S.A.* **2001**, *98*, 7662–7665. (b) Shivanyuk, A.; Rebek, J., Jr. *Chem. Commun.* **2001**, 2424–2425. (c) Avram, L.; Cohen, Y. *J. Am. Chem. Soc.* **2002**, *124*, 15148–15149. (d) Avram, L.; Cohen, Y. *Org. Lett.* **2002**, *4*, 4365–4368. (e) Shivanyuk, A.; Rebek, J., Jr. *J. Am. Chem. Soc.* **2003**, *125*, 3432–3433.

ecules was used to stabilize self-folding container molecules.<sup>7</sup> These also form inclusion complexes with complementary tetraalkylammonium (phosphonium) cations that are stable on the NMR time scale at ambient temperatures. Even steric hindrance has been of use to stabilize calixarene tetraurea capsules in competitive media.<sup>8</sup>

Herein we report the capsular assemblies of pyrogallolarenes **2** in polar protic solvents.<sup>9</sup> We show that the polar solvent molecules assist the assembly of capsular dimers both in solution and in the crystalline state.

## Results and Discussion

**Synthesis and Single-Crystal X-ray Analyses.** Compounds **2** are easily prepared by acid-catalyzed condensation of pyrogallol with the corresponding aldehydes<sup>10</sup> similarly to resorcinolares **1**. Under conditions of thermodynamic control the bowl-shaped all-cis isomers are obtained. Several crystal structures have established that the crown conformation of **2** is stabilized by four intramolecular hydrogen bonds between neighboring pyrogallol rings. Molecules **2** usually cocrystallize with hydrogen-bonding solvent molecules to form infinite chains or layers.<sup>11</sup> The groups of Mattay<sup>11</sup> and Atwood<sup>12</sup> discovered that in the crystalline state pyrogallolarene **2c** forms a spectacular hexameric capsule with a molecular cavity of about 1.5 nm<sup>3</sup>. Water-soluble compound **2e** was shown to form open 1:1 complexes with hydrophobic sugars and nucleotides in aqueous solution.<sup>13</sup>

Slow crystallization of pyrogallolarene **2a** from methanol gave diffraction quality crystals. In the crystalline state a molecule of **2a** adopts a slightly distorted crown conformation that is stabilized by four intramolecular hydrogen bonds (Figure 1). One methanol molecule is included into the concave surface of **2a**. However, the distance between its methyl group and the center of the closest pyrogallol ring (4.1 Å) suggests only a very weak host–guest interaction. Molecules **2a** form infinite sheets through intermolecular hydrogen bonds between the pyrogallol hydroxy groups.

A structure similar to **2a**·5 MeOH was obtained by slow crystallization of long-chain derivative **2d** from EtOH. The molecule of **2d** adopts a bowl-shaped crown conformation in the solid state, stabilized by four intramolecular hydrogen bonds (Figure 2). The remaining hydroxy groups do not form intramolecular hydrogen bonds. Instead, the intermolecular hydrogen bonding occurs between neighboring molecules of **2d** and ethanol molecules. Altogether four ordered ethanol molecules are found, one of which is included in the  $\pi$ -basic cavity of the pyrogallolarene. Four undecyl chains are perfectly

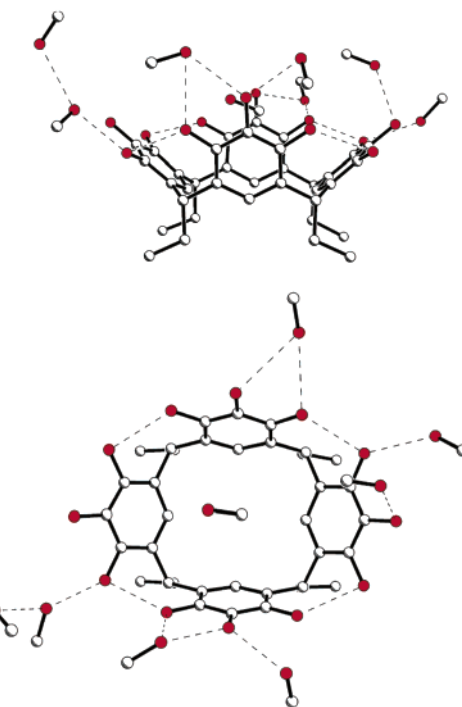


**FIGURE 1.** Single-crystal X-ray structure of **2a**·5 MeOH. Hydrogen bonds are shown as dashed lines. Hydrogen atoms are omitted for clarity.

ordered: three of them are all staggered and one is slightly folded, apparently an imposition of crystal packing forces. The molecules of **2d** pack into bilayers: hydrophobic interactions between their long aliphatic chains represent one layer while the hydroxy groups and ethanol molecules compose the hydrophilic layer.

Recrystallization of compound **2a** from methanol in the presence of quinuclidine hydrochloride **3a**<sup>+</sup> Cl<sup>-</sup> affords diffraction quality crystals. As expected, a molecule of **2a** adopts a perfect crown conformation stabilized by four intramolecular hydrogen bonds. Two molecules of **2a** form a capsule (Figure 3) around one quinuclidinium cation. The 2:1 stoichiometry of the complex was additionally proven by a <sup>1</sup>H NMR spectroscopic study of the crystal redissolved in DMSO-*d*<sub>6</sub>. Due to severe disorder, the nitrogen atoms of the encapsulated cation could not be unambiguously assigned from the electron density map. Eight contacts in the range 3.3–3.4 Å were found between the atoms of the encapsulated cation and the centers of the pyrogallol rings of **2a**, which indicate C–H (N–H)··· $\pi$  host–guest interactions. The quinuclidinium cation (volume 117 Å<sup>3</sup>)<sup>14</sup> occupies about 82% of the available space in the cavity (143 Å<sup>3</sup>).<sup>15</sup> This packing coefficient is much higher than the optimal 55% value for encapsulated neutral molecules<sup>16</sup> in solution. Evidently, strong host–guest interactions in the solid state permit denser packing.<sup>17</sup>

(7) Rafai Far, A.; Shivanyuk, A.; Rebek, J., Jr. *J. Am. Chem. Soc.* **2002**, *124*, 2854–2855.

(8) Vysotsky, M. O.; Thondorf, I.; Boehmer, V. *Chem. Commun.* **2001**, 1890–1891.

(9) For a preliminary communication see: Shivanyuk, A.; Rebek, J., Jr. *Chem. Commun.* **2001**, 2374–2375.

(10) Weinelt, F.; Schneider, H.-J. *J. Org. Chem.* **1991**, *56*, 5527–5535.

(11) Gerkensmeier, T.; Iwanek, W.; Agena, C.; Frolich, R.; Kotila, S.; Nather, C.; Mattay, J. *Eur. J. Org. Chem.* **1999**, 2257–2262.

(12) (a) Atwood, J. L.; Barbour, L. J.; Jerga, A. *Proc. Natl. Acad. Sci. U.S.A.* **2002**, *99*, 4837–4841. (b) Atwood, J. L.; Barbour, L. J.; Agoston, J. *Chem. Commun.* **2001**, 2376–2377.

(13) Kobayashi, K.; Asakawa, Y.; Kato, Y.; Aoyama, Y. *J. Am. Chem. Soc.* **1992**, *114*, 10307–10313.

(14) Web Lab Viewer Pro Version 5, 2000; Molecular Simulation Inc.

(15) DeepView, Swiss PDB Viewer; Guex, N.; Peitsch, M.; Schwede, T.; Diemand, A.; Glaxo Smith Klein.

(16) Mecozzi, S.; Rebek, J., Jr. *Chem. Eur. J.* **1998**, *4*, 1016–1022.

(17) Compare to: (a) Vysotsky, M. O.; Pop, A.; Broda, F.; Thondorf, I.; Böhmer, V. *Chem. Eur. J.* **2001**, *7*, 4403–4410. (b) Thondorf, I.; Broda, B.; Rissanen, K.; Vysotsky, M.; Böhmer, V. *J. Chem. Soc., Perkin Trans. 2* **2002**, 1796–1800.

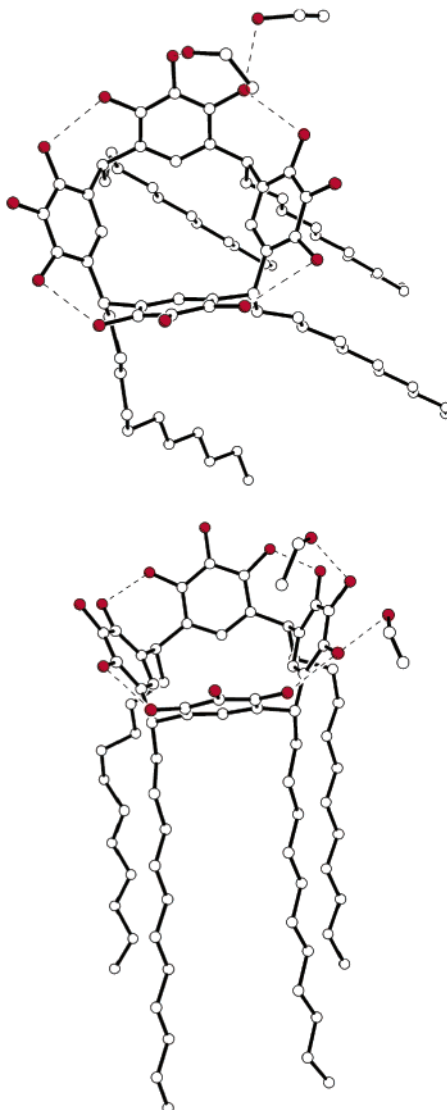


**FIGURE 2.** Single-crystal X-ray structure of **2d**·4EtOH. All hydrogen atoms and two ethanol molecules are omitted for clarity; hydrogen bonds are indicated by dotted lines; top, top view; bottom, side view.

The chloride anion is situated outside of the cavity and is hydrogen bonded to both the hydroxy group of **2a** and the methanol molecules. The shortest distance between the cation and the anion was found to be 6.4 Å, a value about two times longer than in quinuclidine hydrochloride itself.<sup>18</sup> This is a rare example of a capsule-separated ion pair in the crystalline state.<sup>19</sup> The energy of the charge separation is apparently compensated by the strong host–guest interaction and the hydrogen-bonding solvation of the highly polar chloride anion. The capsule is held together by a complicated array of hydrogen bonds, which includes direct hydrogen bonding between the hydroxy groups of **2a** and bridging of the hydroxy groups by methanol and water molecules. Altogether one water and seven methanol molecules participate in the

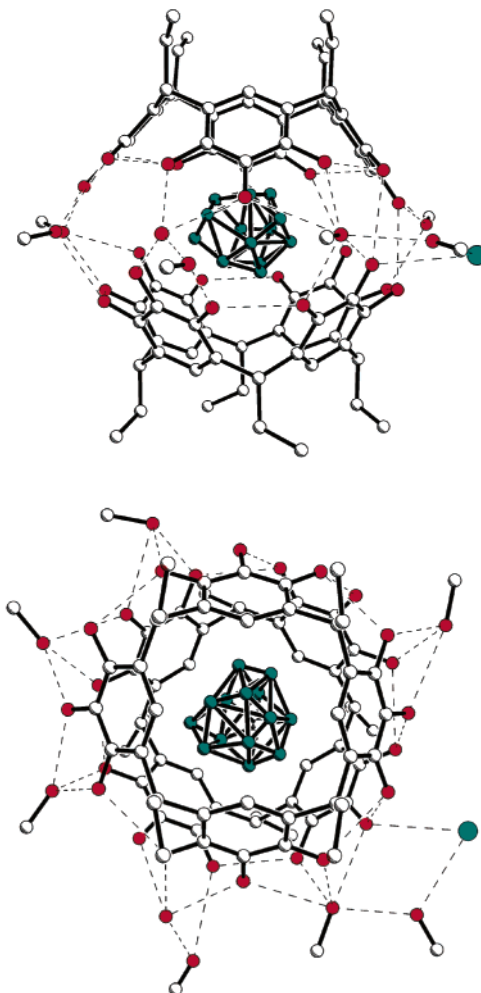


**FIGURE 3.** Single-crystal X-ray structure of **2a**<sub>2</sub>·3a<sup>+</sup>Cl<sup>-</sup>·7MeOH·H<sub>2</sub>O. Hydrogen bonds are shown as dashed lines and hydrogen atoms are omitted for clarity. The chloride anion is shown as a green sphere. The disordered cation is shown as blue spheres.

formation of the capsule. As seen in Figure 3, the capsular assembly has no plane or center of symmetry and is therefore chiral. Both enantiomers are present in the unit cell. They are related by inversion center in space group *P*2<sub>1</sub>/n showing that the crystal is a racemate.

Pyrogallolarene **2b** is not soluble in dry acetonitrile. However, the addition of a small amount of water and heating results in its dissolution. After 10 h at room temperature, colorless, transparent crystals grew which were of suitable size and quality for single-crystal X-ray analysis.

The molecule of **2b** adopts a slightly distorted crown conformation stabilized by four intramolecular hydrogen bonds between the neighboring pyrogallol rings. Two molecules of **2b** form a centrosymmetrical (space group *P*1) capsular dimer (Figure 4) with a cavity of 277 Å<sup>3</sup>. The polar belt of the capsule is composed of 12 hydroxy groups of the two molecules **2b** and 16 hydrogen-bonded water molecules. Four acetonitriles are found inside the cavity—an unprecedented number of guests for a dimeric capsular host. Two acetonitrile molecules have their methyl groups pointing toward the π-basic cavities of molecules **2b**. The distances between the methyl carbon

(18) Kurahashi, M.; Engel, P.; Nowacki, W. *Z. Kristallogr., Kristallgeom., Kristallphys., Kristallchem.* **1980**, *152*, 147.

(19) (a) Shivanyuk, A.; Paulus, E. F.; Bohmer, V. *Angew. Chem., Int. Ed.* **1999**, *38*, 2906–2909. (b) Shivanyuk, A.; Rissanen, K.; Kolehmainen, E. *Chem. Commun.* **2000**, 1107–1108.

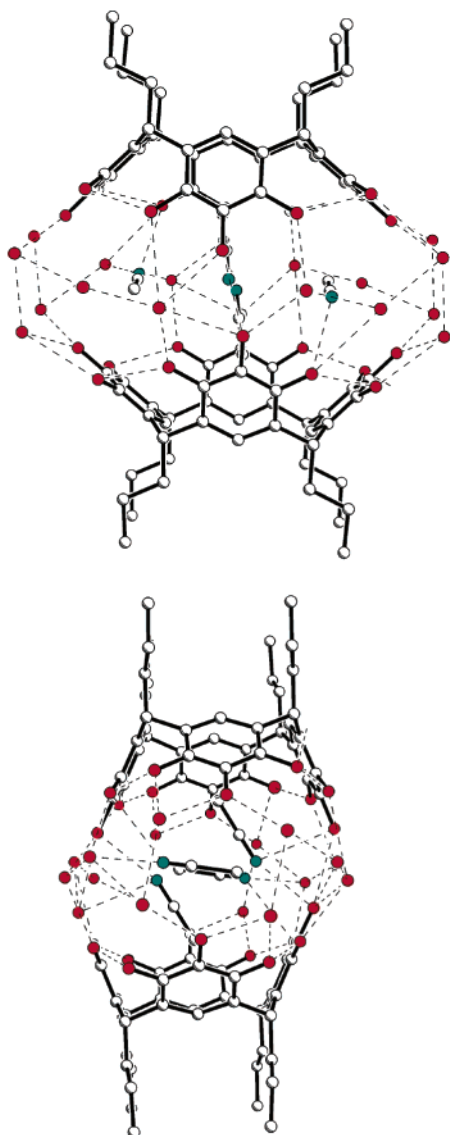


**FIGURE 4.** The X-ray structure of **2b**·3 MeCN·5 H<sub>2</sub>O. Symmetry-related water molecules are shown. Hydrogen atoms are omitted for clarity and heteroatoms are darkened. Hydrogen bonds are indicated as dashed lines. Acetonitrile molecules positioned outside the cavity are not shown. Only one position of the disordered acetonitriles is indicated.

atoms and the centers of the closest aromatic rings are 3.4 Å and indicate some CH- $\pi$  attractions. The nitrogens appear to form three-centered hydrogen bonds with the hydroxyls of **2b**. Two short intermolecular contacts between carbon and nitrogen atoms of the nitrile groups (3.4 Å) and their antiparallel orientation indicates likely dipole-dipole interactions. The fact that these acetonitrile molecules are not disordered indicates a considerable energetic advantage of the orientation shown compared to any other. The other two acetonitrile molecules are nearly parallel to the planes of the methine bridges of **2b**. They form hydrogen bonds with the pyrogallol hydroxy groups and the water molecules are disordered over two positions with an occupancy factor of 0.5. Most probably, this slight disorder reflects a very small energy difference between the two orientations. The packing coefficient of the capsule shown in Figure 3 is 63%—much

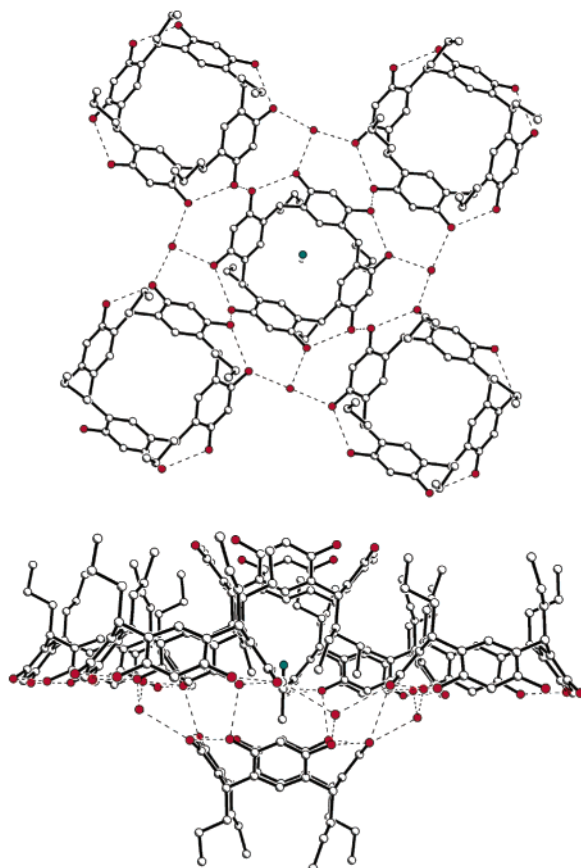


**FIGURE 5.** Packing diagram of the crystal structure **1c**·MeCN·4 H<sub>2</sub>O: top, top view (five molecules of **1c** are shown); bottom, side view (six molecules of **1c** are shown). Hydrogen bonds are shown by dashed lines. Some water molecules are omitted for clarity.

higher than the value of liquid acetonitrile (51.0% at 293 K). This is in accordance with the highly ordered (solid) state of the acetonitrile molecules.

Slow recrystallization of resorcinarene **1c** from aqueous acetonitrile results in colorless prismatic crystals. Single-crystal X-ray analysis reveals that the molecule of **1c** exists in a perfect crown conformation stabilized by hydrogen bonds between the hydroxy groups of neighboring resorcinol rings (Figure 5). Four hydroxy groups of **1c** form hydrogen bonds to four water molecules in a chiral *C*<sub>4</sub>-symmetrical manner, but the structure is centrosymmetric (space group *P*4/n). A molecule of **1c** is hydrogen bonded to four other molecules of **1c** that results in a cyclic hydrogen-bonding array and in the extension of the cavity (Figure 5, top).<sup>20</sup> This cavity is closed on the top by another molecule of **1c** (Figure 5, bottom) and one acetonitrile molecule is included inside.

The different types of crystal structures formed by **1c** and **2b** obtained under the same conditions indicate that the presence of the four additional hydroxy groups in molecule **2b** is responsible for the formation of the water-linked, dimeric molecular capsule in the crystalline state.

Crystallization of **1d** from methanol at 273 K results in prism-like crystals suitable for crystallographic stud-

(20) For a similar arrangement see: Atwood, J. L.; Barbour, L. J.; Ness, T. J.; Raston, C. L.; Raston, P. L. *J. Am. Chem. Soc.* **2001**, *123*, 7192–7193.

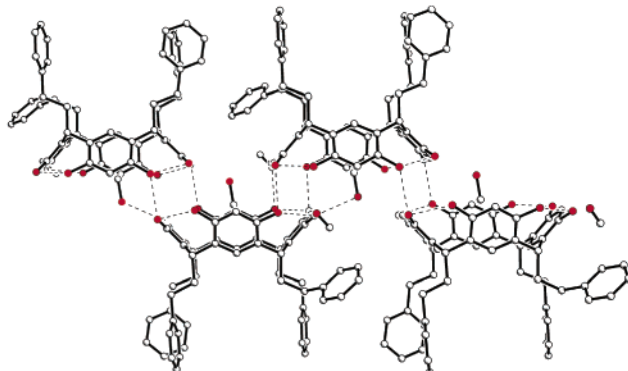


**FIGURE 6.** Part of the infinite hydrogen-bonded chains of **1d** in the crystalline state. Hydrogen bonds are indicated by dashed lines. Hydrogen atoms are omitted for clarity.

ies. Again, the molecule of **1d** exists in a crown conformation stabilized by intramolecular hydrogen bonds. Infinite “oscillating” chains form through intermolecular hydrogen bonds between the resorcinol hydroxy groups (Figure 6). Two methanol molecules are hydrogen bonded to each molecule of **1d** and assume well-defined positions. The concave surface of **1d** hosts the methyl group of a methanol molecule.

**Reversible Encapsulation in Solution.** The  $^1\text{H}$  NMR spectrum of **2a** measured in methanol- $d_4$  at 303 K is sharp and contains one triplet for the methine protons of the bridges and one singlet for the protons of the pyrrogallol rings. This pattern is characteristic of the  $C_{4v}$ -symmetrical crown conformation found in the crystalline state. Decreasing the temperature to 223 K does not result in considerable spectral changes. The crown conformation of **2a** is stable on the NMR time scale and the pattern observed is not caused by the fast interconversion between two  $C_{2v}$ -symmetrical boat conformers.<sup>21</sup> The  $^1\text{H}$  NMR spectrum of **2a** in methanol- $d_3$  does not show any indication of strong interactions with solvent molecules between 295 and 223 K. Two broad signals were observed at 295 K for hydroxy groups at 8.6 and 7.8 ppm in a 2:1 ratio (Figure 7a). Decreasing the temperature to 223 K slows down the exchange of the hydroxyl protons and gives rise to four major sharp resonances for the hydroxy groups and a set of minor signals (Figure 7b). Apparently, several pyrrogallolarenes with different symmetry of hydrogen-bonding arrays coexist. Three such arrangements allow four intramolecular hydrogen bonds (Figure 8) and should have comparable energies. Surprisingly, the  $^1\text{H}$  NMR spectrum of resorcinarene **1b** at 223 K contained only one OH signal, indicating fast exchange between the different hydrogen-bonding arrangements (Figure 7c).

The crystal structure of  $\mathbf{2a}_2 \cdot \mathbf{3a}^+ \text{Cl}^- \cdot 7 \text{ MeOH} \cdot \text{H}_2\text{O}$  (Figure 3) suggested that pyrrogallolarenes might form dimeric capsules in alcohols. The addition of  $\mathbf{3a}^+ \text{Cl}^-$  to the solution of **2a** in methanol- $d_4$  did not significantly change the  $^1\text{H}$  NMR spectrum of the pyrrogallolarenne at

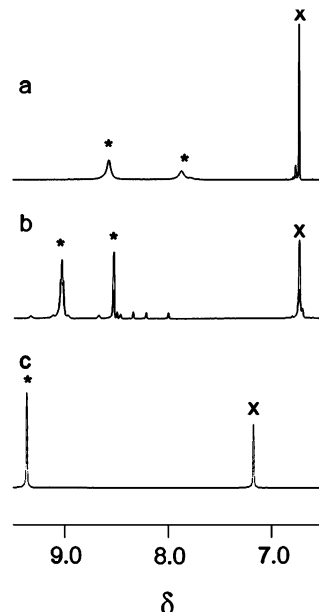


**FIGURE 7.**  $^1\text{H}$  NMR spectra (600 MHz, methanol- $d_3$ ): (a) **2a** at 303 K; (b) **2a** at 223 K; (c) **1b** at 223 K. Key: \*, OH protons; X, protons in 5-positions of the resorcinol ring.

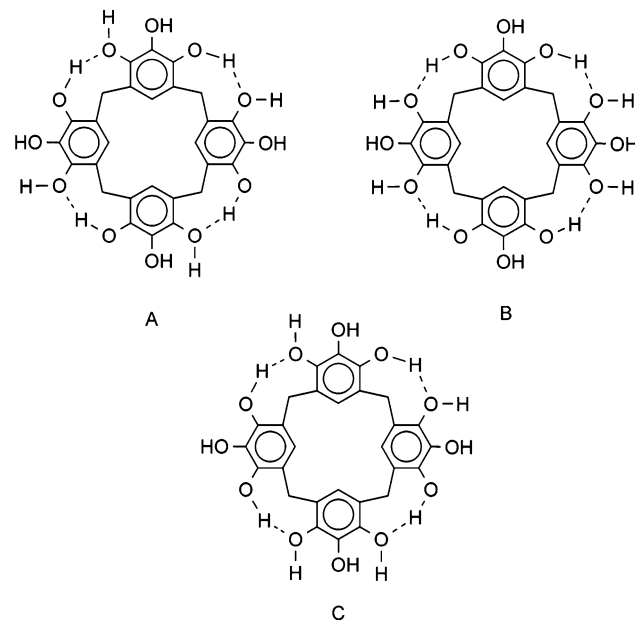


**FIGURE 8.** Three possible arrangements with four intramolecular hydrogen bonds.

295 K. Very broad signals were detected for the protons of  $\mathbf{3a}^+$  indicating the formation of a complex that is exchanging fast with its components on the NMR time scale. Decreasing the temperature to 253 K gave rise to the sharper signals of the complexed cation; however, the guest exchange was still fast on the NMR time scale (Figure 9a). At 223 K exchange became slow and dilution experiments revealed that one cation is complexed by two molecules of **2a** (Figure 9b, right). The induced chemical shift ( $\Delta\delta$ ) for the resonance of the methine proton  $\mathbf{3a}^+$  is  $-4.01$  ppm and places it in proximity to the shielding regions of the host. The methylene protons of the cation are much less shielded ( $\Delta\delta = -3.22$  and  $-3.41$  ppm),

(21) (a) Höglberg, A. G. S. *J. Am. Chem. Soc.* **1980**, *102*, 6046–6050. (b) Höglberg, A. G. S. *J. Org. Chem.* **1980**, *45*, 4498–4500. (c) Abis, L.; Dalcanale, E.; Du vose, A.; Spera, S. *J. Chem. Soc., Perkin Trans. 2* **1990**, 2075–2080. (d) Abis, L.; Dalcanale, E.; Du vose, A.; Spera, S. *J. Org. Chem.* **1988**, *53*, 5475–5479. (e) Shivanayuk, A. N.; Pirozhenko, V. V.; Kalchenko, V. I.; Markovsky, L. N. *J. Chem. Res. (S)* **1995**, 374–375.

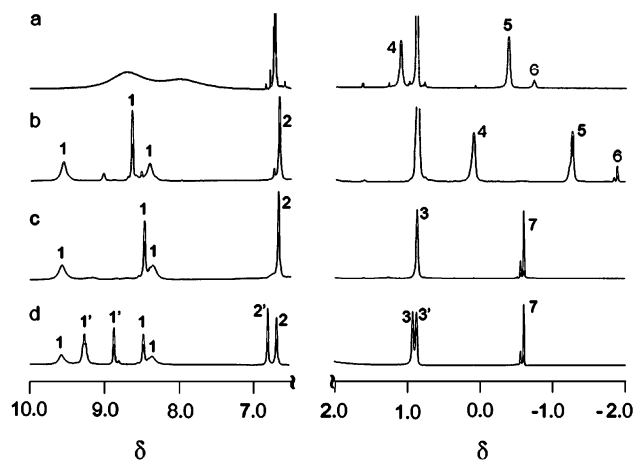


**FIGURE 9.**  $^1\text{H}$  NMR spectra in (600 MHz) methanol- $d_4$ : (a)  $2\mathbf{2a} + 3\mathbf{a}^+ \text{Cl}^-$  at 243 K; (b)  $2\mathbf{2a} + 3\mathbf{a}^+ \text{Cl}^-$  at 223 K; (c)  $2\mathbf{2a} + 3\mathbf{a}^+ \text{Br}^-$  at 223 K; (d)  $2\mathbf{2a} + 1.5\mathbf{3a}^+ \text{Br}^-$  at 223 K. Key: 1 and 1', OH protons in capsular and open ended complex, respectively; 2 and 2', protons of the pyrogallol rings in capsular and open ended complex, respectively; 3 and 3', methyl protons of pyrogallolarene in capsular and open ended complex, respectively; 4,  $\text{NCH}_2$  protons of  $3\mathbf{a}^+$ ; 5,  $\text{NCH}_2\text{CH}_2$  protons of  $3\mathbf{a}^+$ ; 6, CH protons of  $3\mathbf{a}^+$ ; 7, protons of  $3\mathbf{b}^+$ .

indicating that, on average, the  $C_3$  axis of  $3\mathbf{a}^+$  is oriented along the smaller axis of the capsule. Three singlets were detected for the hydroxyl protons in a 1:1:1 ratio while one triplet and one singlet correspond to the methine protons of the bridges and aromatic protons of the pyrogallol rings (Figure 9b, left). This pattern corresponds to the  $C_4$ -symmetrical chiral arrangement A (Figure 8). The dimerization of two molecules of  $\mathbf{2a}$  having such an arrangement should result in two diastereomeric capsules having the same or opposite handedness of the hydrogen-bonding arrays. The fact that two close signals (1:4 ratio) were detected for the methine protons of encapsulated  $3\mathbf{a}^+$  (Figure 9b, right) may indicate formation of diastereomeric capsules (see discussion below).

In contrast, triethylammonium cation  $3\mathbf{d}^+$  ( $121\text{ \AA}^3$ ), which is the same size as  $3\mathbf{a}^+$  ( $119\text{ \AA}^3$ ), was not encapsulated by the dimeric capsule of  $\mathbf{2a}$  in methanol. The spectrum of a solution containing  $\mathbf{2a}$  and  $3\mathbf{d}^+$  in a 2:1 molar ratio reveals relatively weak upfield shifts for the methyl (0.6 ppm) and methylene (0.9 ppm) protons of the cation. This indicates the formation of an open monomeric complex that is in fast exchange with its components. The distance between the methyl groups of  $3\mathbf{d}^+$  (4.4 Å) is about 1.7 times longer than the distance between the nitrogen and methine carbon atom of  $3\mathbf{a}^+$ . Thus, the compact shape rather than the volume determines the selectivity of encapsulation in the pyrogallolarene dimeric capsule.

Tetramethylammonium and tetramethylphosphonium cations ( $3\mathbf{b}^+$  and  $3\mathbf{c}^+$ ) are also encapsulated by the dimer of  $\mathbf{2a}$  in methanol- $d_4$ . At 303 K the  $^1\text{H}$  NMR spectrum contains very broad signals for the cations indicating complexation that is fast on the NMR time scale. The signals become sharper upon cooling to 253 K; however, the complex is still kinetically unstable. Further decrease of the temperature results in a gradual upfield shift of the resonances of the encapsulated cations. Below 233

K their chemical shifts do not change and the exchange becomes slow on the NMR time scale. In the presence of 4 equiv of  $\mathbf{2a}$  per equivalent of the salt, the signals of both free and complexed pyrogallolarene are found in a 1:1 ratio. The integration of the spectra reveals that a dimeric capsule is formed that contains one cation. The strong upfield shift of the protons of  $3\mathbf{b}^+$  ( $\Delta\delta = -4.3$  ppm) also indicates that the complex formed has a dimeric capsular structure. Three singlets for the OH protons were observed in the downfield window of the  $^1\text{H}$  NMR spectrum at 223 K (Figure 9c), similar to the capsule with  $3\mathbf{a}^+$  (see above). The presence of two singlets for the methyl protons of the encapsulated cation  $3\mathbf{b}^+$  indicates formation of slightly different diastereomeric capsules. Analogous behavior was also observed for the capsular assembly with tetramethylphosphonium cation  $3\mathbf{c}^+$ . Two doublets are detected for the protons of the encapsulated cation (4:1 ratio) at 223 K that are shifted upfield by about 4.0 ppm. Two resonances in a 4:1 ratio were observed in the  $^{31}\text{P}$  NMR spectrum for the phosphorus atoms of encapsulated  $3\mathbf{c}^+$ .

The  $^{19}\text{F}$  NMR spectrum of the capsular complex with  $3\mathbf{b}^+ \text{BF}_4^-$  at 223 K in methanol- $d_4$  contains only the signal for the free anion, confirming that only the cation is encapsulated. Accordingly, the mixing of capsular complexes of  $3\mathbf{b}^+ \text{Cl}^-$  and  $3\mathbf{b}^+ \text{Br}^-$  reveals the fast exchange of the anions.

The addition of  $3\mathbf{b}^+ \text{Br}^-$  to the solution of the capsule gives rise to a new set of signals for the protons of pyrogallolarene (Figure 9d). The original capsule resonances continue to decrease as more salt is added. Upon addition of 3 equiv of the salt almost no capsule can be detected. The signal of the excess salt is broadened and shifted upfield relative to its normal position. The chemical shift of this signal depends on the amount of the guest added, indicating formation of a kinetically unstable open complex.<sup>22</sup>

The spectrum of tropylidium tetrafluoroborate  $4^+ \text{BF}_4^-$  in methanol- $d_4$  at 295 K reveals one very broad signal at 9.2 ppm due to some exchange process that is slow on the NMR time scale (Figure 10a). At 233 K the spectrum contains one sharp singlet at 9.2 ppm for the tropylidium cation and three sharp multiplets (1:1:1 ratio) corresponding to a new species (Figure 10b). A 1D GOESY experiment with the tropylidium resonance suppressed reveals that the tropylidium cation is in equilibrium with the other species. This is most probably caused by reversible methanolysis of the tropylidium cation giving methoxycycloheptatriene and  $\text{HBF}_4$  (Scheme 1).<sup>23</sup>

The addition of pyrogallolarene  $\mathbf{2a}$  to a solution of  $4^+ \text{BF}_4^-$  in methanol- $d_4$  results in an intense red color ( $\lambda = 407\text{ nm}$ )<sup>24</sup> that manifests a charge-transfer host-guest interaction. The  $^1\text{H}$  NMR spectrum in the presence of 4 equiv of  $\mathbf{2a}$  measured at 295 K contains a broadened  $C_{4v}$  symmetrical pattern for the protons of pyrogallolare-

(22) (a) Murayama, K.; Aoki, K. *Chem. Commun.* **1997**, 119–120. (b) Lipmann, T.; Wilde, H.; Pink, A.; Schäfer, M.; Hesse, M.; Mann, G. *Angew. Chem., Int. Ed. Engl.* **1993**, 32, 1195–1197. (c) Shivanyuk, A.; Paulus, E. F.; Rissanen, K.; Böhmer, V. *Chem. Eur. J.* **2001**, 7, 1944–1951.

(23) (a) von E. Doering, W.; Knox, L. H. *J. Am. Chem. Soc.* **1954**, 76, 3203–3206. (b) Mayr, H.; Müller, K.-H.; Ofial, A. R.; Buhl, M. *J. Am. Chem. Soc.* **1999**, 121, 2418–2424.

(24) See for example: Lämsä, M.; Pursiainen, J.; Rissanen, K.; Huuskonen, J. *Acta Chem. Scand.* **1998**, 52, 563–570.

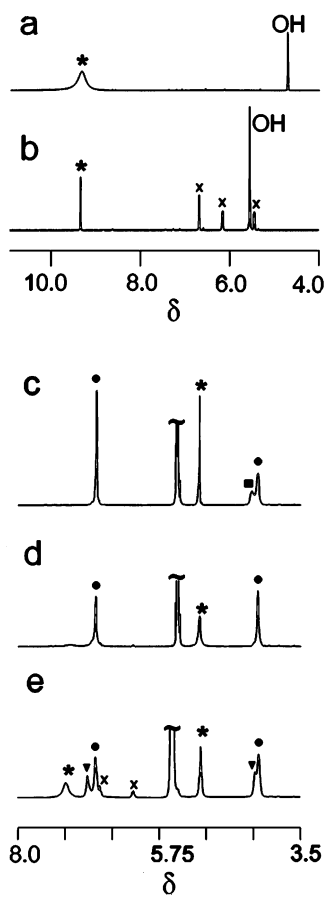
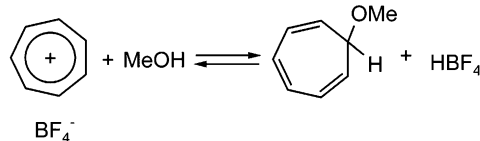


**FIGURE 10.**  $^1\text{H}$  NMR spectra (600 MHz, methanol- $d_4$ ,  $[\mathbf{1a}]_{\text{total}} = 2 \text{ mM}$ ): (a)  $\text{C}_7\text{H}_7^+ \text{BF}_4^-$  at 295 K; (b)  $\text{C}_7\text{H}_7^+ \text{BF}_4^-$  at 233 K; (c) 4  $\mathbf{1a}$  +  $\text{C}_7\text{H}_7^+ \text{BF}_4^-$  at 233 K; (d) 2  $\mathbf{2a}$  +  $\text{C}_7\text{H}_7^+ \text{BF}_4^-$  at 223 K; (e)  $\mathbf{2a}$  +  $\text{C}_7\text{H}_7^+ \text{BF}_4^-$  at 233 K. Key: \*, tropylium cation; □, free  $\mathbf{2a}$ ; ●,  $\mathbf{2a}$  in 2:1 complex; ▼,  $\mathbf{2a}$  in an open complex; ×, methoxycycloheptatriene.

**SCHEME 1**



ne and a sharp singlet at 5.2 ppm for the protons of the complexed tropylium cation. Lowering the temperature to 233 K results in the splitting of the signal for the methine protons of  $\mathbf{2a}$  (Figure 10c) while the signal of the complexed tropylium cation maintains its shape and position. This indicates that the complex is stable on the NMR time scale at 233 K. Dilution experiments revealed that one tropylium cation is complexed by two pyrrogallolarenes ( $\mathbf{2a}$ ) (Figure 10d), while the strong shielding of the tropylium protons suggests that a capsular assembly is formed.<sup>19a</sup> The encapsulation provides a supramolecular protection for the tropylium cation since no methanolysis was detected in the solution at  $[\mathbf{2a}]/[\mathbf{4}^+ \text{BF}_4^-] \geq 2$ . The addition of  $\mathbf{4}^+ \text{BF}_4^-$  to a solution of 2  $\mathbf{2a} \cdot \mathbf{4}^+ \text{BF}_4^-$  gives rise to a new set of signals for the protons of  $\mathbf{2a}$  that grows at the expense of the set for the 2:1 complex (Figure 10e). Finally, when 4 equiv of  $\mathbf{4}^+ \text{BF}_4^-$  is added, no dimeric complex was observed. Remarkably, no signals for the free tropylium cation were

detected for host:guest ratios less than 2. Instead, a broad resonance emerged, whose chemical shift depended on the concentration of the tropylium salt. This suggests that the new set of signals corresponds to an open, presumably 1:1, complex between the tropylium cation and  $\mathbf{2a}$ , in fast exchange with its components.<sup>25</sup> The NMR spectroscopy revealed that such a complexation *does not* inhibit the methanolysis of the tropylium cation (Scheme 1).

Dimeric pyrrogallolarenes encapsulate ions  $\mathbf{3a}^+ \cdot \mathbf{c}^+$  and  $\mathbf{4}^+$  in ethanol, 2-propanol, and aqueous acetonitrile. In the latter case the binding studies are somewhat hampered by precipitation of ice at lower temperatures. Hydrogen bonding with alcohol molecules is required for the formation of the dimeric capsules. Lipophilic pyrrogallolarenes  $\mathbf{2d}$  exists in  $\text{CDCl}_3$  as a giant hexameric capsule.<sup>26</sup> Cations  $\mathbf{3a} \cdot \mathbf{c}^+$  and  $\mathbf{4}^+$  are not encapsulated when added to this solution. However, the addition of small amounts of methanol- $d_4$  (ca. 10%) results in the formation of the dimeric capsules similar to those found in pure methanol. The addition of ethanol and 2-propanol also resulted in encapsulation of the cations.

The addition of tetramethylammonium and phosphonium bromides does not significantly change the  $^1\text{H}$  NMR spectrum of resorcinarene  $\mathbf{1a}$  in methanol- $d_4$  at 295 K. The signals for  $\mathbf{3b}^+$  ( $\mathbf{3c}^+$ ) were shifted upfield by 0.68 ppm, in the presence of 2 equiv of  $\mathbf{1a}$ . Decreasing the temperature to 233 K did not change the patterns for the protons of  $\mathbf{1a}$ . However, the signal for  $\mathbf{3b}^+$  became broad and shifted further upfield by 0.3 ppm. In the case of tetramethylphosphonium bromide, the spectrum at 233 K contains a sharp doublet for the cation at 0.69 ppm ( $\Delta\delta = -1.2$  ppm). The induced chemical shifts of  $\mathbf{3b}^+$  and  $\mathbf{3c}^+$  depended on the amount of host  $\mathbf{1a}$  in solution while the variable-temperature dilution experiments reveal that the complexes are not stable on the NMR time scale between 295 and 233 K. This suggests the formation of an open-ended 1:1 complex similar to those found in the crystalline state.<sup>22</sup> Tropylium cation  $\mathbf{4}^+$  also forms analogous weak complexes with  $\mathbf{1a}$  in methanol- $d_4$  that give a characteristic red color to the solution. At 233 K the set of signals for the methanolysis product was observed simultaneously with the averaged peak of the free and complexed tropylium cation. This indicates that the formation of the open complex between  $\mathbf{4}^+$  and resorcinarene does not prevent the reaction shown in Scheme 1.

The concavities of pyrrogallolarenes  $\mathbf{2}$  are more  $\pi$ -basic than those of resorcinarenes  $\mathbf{1}$  and should cause stronger interactions between  $\mathbf{2}$  and cationic guests. The formation of capsular dimers of  $\mathbf{2}$  is further facilitated by direct hydrogen bonding between hydroxy groups as shown in the crystalline state (see Figure 3).

The interaction between pyrrogallolarenes  $\mathbf{2a}$  and guests  $\mathbf{3a}^+ \cdot \mathbf{c}^+$  and  $\mathbf{4}^+$  persists in the gas phase. Typically, the negative ion ESI mass spectrum of methanol solutions of the complex contains peaks at 664 and 1328 D corresponding to the monomer and the dimer of  $\mathbf{2a}$ . The

(25) About analogous behavior of capsular complexes see: Frish, L.; Vysotsky, M. O.; Matthews, S. E.; Boehmer, V.; Cohen, Y. *J. Chem. Soc., Perkin Trans. 2* **2002**, 88–93.

(26) This was shown by studies of diffusion coefficients: Palmer, L.; Shivanyuk, A.; Rebek, Jr., J. Unpublished results.

positive ion spectrum contains peaks of monomeric complexes **2a**  $\subset$  **3a-c(4)<sup>+</sup>** and the dimers **2 2a**  $\subset$  **3(4)<sup>+</sup>**. No peaks for the 2:1 complexes including solvent molecules were observed indicating that weakly interacting solvent molecules are lost during the ionization procedure. The peaks corresponding to the 2:1 complexes with guests **3a-c<sup>+</sup>** and **4<sup>+</sup>** were also detected for resorcinarenes **1b** from methanol solution.<sup>27</sup>

## Conclusion

In conclusion, readily available pyrrogallolarenes **2** dimerize in the presence of suitable charged guests and give hydrogen-bonded molecular capsules that are highly stable in competing solvents such as alcohols. The solvent molecules participate in the capsular assemblies as linkers that cooperate with the direct hydrogen bonds between pyrrogallolarene hemispheres. Strong cation- $\pi$  and charge-transfer interactions between guests and the  $\pi$ -basic pyrrogallol rings of **2** make considerable contributions to the overall stability of the dimeric assemblies. Crystallographic and spectroscopic studies revealed that the capsular complexes of **2** and **3a-c<sup>+</sup>** are encapsulation-separated ion pairs, i.e., only cations are surrounded by the capsules while the anions remain outside. The energy necessary for the charge separation is likely compensated by strong host/guest interactions. The encapsulation of the tropylium cation is accompanied by the characteristic change of color that is caused by charge-transfer host-guest interactions. The closed dimeric shell prevents the reversible alcoholysis of the encapsulated tropylium cation, demonstrating an example of supramolecular protection of a relatively reactive species.

## Experimental Section

**General Methods and Technique.** NMR spectra were recorded on a Bruker DRX 600 (600 MHz) spectrometer, using the solvent signals as internal reference. Electrospray ionization (ESI) mass spectra were recorded on an API III Perkin-Elmer SCIEX triple quadrupole mass spectrometer. All guests were purchased from Aldrich and Fluka and were used without further purification. Compounds **1**<sup>28</sup> and **2**<sup>10</sup> were prepared by known procedures.

**Single-Crystal X-ray Analyses.** Crystallographic data were collected on a Siemens SMART<sup>29</sup> diffractometer equipped with a CCD area detector, using graphite monochromatized Mo K $\alpha$  radiation [ $\lambda$ (Mo K $\alpha$ ) = 0.71073 Å]. Data in the frames corresponding to an arbitrary hemisphere of data were integrated with SAINT.<sup>30</sup> Data were corrected for Lorentz and polarization effects and were further analyzed by using XPREP. An empirical absorption correction based on the measurement of redundant and equivalent reflections and an

(27) Compare with: Mansikkamaki H.; Nissinen, M.; Schalley C. A.; Rissanen, K. *New J. Chem.* **2003**, *27*, 88-97.

(28) Tunstad, L. M.; Tucker, J. A.; Dalcanale, E.; Weiser, J.; Bryant, J. A.; Sherman, J. C.; Helgeson, R. C.; Knobler, C. B.; Cram, D. J. *J. Org. Chem.* **1989**, *54*, 1305-1312.

(29) SMART, Area Detector Software Package; Siemens Industrial Automation, Inc.: Madison, WI, 1995.

(30) SAINT, SAX, Area Detector Integration Program Version 4.024; Siemens Industrial Automation, Inc.: Madison, WI, 1995.

ellipsoidal model for the absorption surface was applied with use of SADABS. The structure solution and refinement were performed with SHELXTL<sup>31</sup> (refining on  $F^2$ ).

**2a-5 MeOH:** measurements at 295 crystal size  $0.3 \times 0.3 \times 0.3$  mm<sup>3</sup>, triclinic,  $P\bar{1}$ ,  $a = 12.657(1)$  Å,  $b = 12.964(1)$  Å,  $c = 14.718(1)$  Å,  $\alpha = 64.575(2)$ °,  $\beta = 80.253(2)$ °,  $\gamma = 80.547(2)$ °,  $V = 2138.4(3)$  Å<sup>3</sup>,  $Z = 2$ ,  $\rho_{\text{calcd}} = 0.958$  g cm<sup>-3</sup>,  $2\Theta_{\text{max}} = 56.12$ °,  $\mu = 0.073$  mm<sup>-1</sup>,  $F(000) = 656$ , 548 parameters,  $R1 = 0.074$ ,  $wR2 = 0.1439$  (for 4120 reflections,  $I > 2\sigma(I)$ ),  $R1 = 0.0925$ ,  $wR2 = 0.1933$  (for 10122 unique reflections),  $S = 0.925$ ,  $\Delta\rho(\text{min/max}) = -0.36/0.40$  e Å<sup>-3</sup>.

**2d-4 EtOH:** crystal size  $0.5 \times 0.3 \times 0.25$  mm<sup>3</sup>, triclinic,  $P\bar{1}$ ,  $a = 11.157(3)$  Å,  $b = 16.173(4)$  Å,  $c = 23.393(7)$  Å,  $\alpha = 108.86$ °,  $\beta = 91.14(1)$ °,  $\gamma = 96.11(1)$ °,  $V = 3964(2)$  Å<sup>3</sup>,  $Z = 2$ ,  $\rho_{\text{calcd}} = 1.067$  g cm<sup>-3</sup>,  $2\Theta_{\text{max}} = 56.12$ °,  $\mu = 0.069$  mm<sup>-1</sup>,  $F(000) = 1408$ , 892 parameters,  $R1 = 0.0580$ ,  $wR2 = 0.1396$  (for 7857 reflections,  $I > 2\sigma(I)$ ),  $R1 = 0.0864$ ,  $wR2 = 0.1583$  (for 12139 unique reflections),  $S = 1.037$ ,  $\Delta\rho(\text{min/max}) = -0.57/0.58$  e Å<sup>-3</sup>.

**2a<sub>2</sub>·3a<sup>+</sup>·Cl<sup>-</sup>·7 MeOH·H<sub>2</sub>O:** measurements at 295 crystal size  $0.3 \times 0.3 \times 0.3$  mm<sup>3</sup>, monoclinic,  $P2_1/n$ ,  $a = 16.26(4)$  Å,  $b = 24.57(7)$  Å,  $c = 22.96(6)$  Å,  $\beta = 93.32(6)$ °,  $V = 9155(44)$  Å<sup>3</sup>,  $Z = 8$ ,  $\rho_{\text{calcd}} = 1.234$  g cm<sup>-3</sup>,  $2\Theta_{\text{max}} = 56.12$ °,  $\mu = 0.122$  mm<sup>-1</sup>,  $F(000) = 3594$ , 1111 parameters,  $R1 = 0.094$ ,  $wR2 = 0.240$  (for 5106 reflections,  $I > 2\sigma(I)$ ),  $R1 = 0.270$ ,  $wR2 = 0.336$  (for 17149 unique reflections),  $S = 0.923$ ,  $\Delta\rho(\text{min/max}) = -0.38/0.77$  e Å<sup>-3</sup>.

**2b<sub>3</sub>·MeCN·5 H<sub>2</sub>O:** measurements at 173.0(2) crystal size  $0.4 \times 0.3 \times 0.3$  mm<sup>3</sup>, triclinic,  $P\bar{1}$ ,  $a = 11.455(1)$  Å,  $b = 11.627$  (1) Å,  $c = 18.662(2)$  Å,  $\alpha = 102.785(2)$ °,  $\beta = 90.042(2)$ °,  $\gamma = 102.881(2)$ °,  $V = 2360.0(4)$  Å<sup>3</sup>,  $Z = 2$ ,  $\rho_{\text{calcd}} = 1.303$  g cm<sup>-3</sup>,  $2\Theta_{\text{max}} = 56.12$ °,  $\mu = 0.1$  mm<sup>-1</sup>,  $F(000) = 984$ , 639 parameters,  $R1 = 0.0620$ ,  $wR2 = 0.1786$  (for 7603 reflections,  $I > 2\sigma(I)$ ),  $R1 = 0.091$ ,  $wR2 = 0.2055$  (for 11082 unique reflections),  $S = 1.057$ ,  $\Delta\rho(\text{min/max}) = -0.62/0.56$  e Å<sup>-3</sup>.

**1c·MeCN·4 H<sub>2</sub>O:** measurements at 295 crystal size  $0.4 \times 0.3 \times 0.3$  mm<sup>3</sup>, tetragonal,  $P4/n$ ,  $a = 14.515(1)$  Å,  $c = 9.3463$  (8) Å,  $V = 1969.2(2)$  Å<sup>3</sup>,  $Z = 8$ ,  $\rho_{\text{calcd}} = 1.204$  g cm<sup>-3</sup>,  $2\Theta_{\text{max}} = 56.04$ °,  $\mu = 0.084$  mm<sup>-1</sup>,  $F(000) = 3594$ , 142 parameters,  $R1 = 0.059$ ,  $wR2 = 0.1737$  (for 1970 reflections,  $I > 2\sigma(I)$ ),  $R1 = 0.068$ ,  $wR2 = 0.1842$  (for 2386 unique reflections),  $S = 1.052$ ,  $\Delta\rho(\text{min/max}) = -0.4/0.74$  e Å<sup>-3</sup>.

**1d<sub>2</sub>·2 EtOH:** measurements at 295 crystal size  $0.3 \times 0.3 \times 0.3$  mm<sup>3</sup>, triclinic,  $P\bar{1}$ ,  $a = 11.663(3)$  Å,  $b = 14.711(3)$  Å,  $c = 15.699(3)$  Å,  $\alpha = 98.691(4)$ °,  $\beta = 91.894(4)$ °,  $\gamma = 102.227(4)$ °,  $V = 2596.2(9)$  Å<sup>3</sup>,  $Z = 2$ ,  $\rho_{\text{calcd}} = 1.240$  g cm<sup>-3</sup>,  $2\Theta_{\text{max}} = 56.04$ °,  $\mu = 0.083$  mm<sup>-1</sup>,  $F(000) = 1032$ , 661 parameters,  $R1 = 0.0683$ ,  $wR2 = 0.1162$  (for 4117 reflections,  $I > 2\sigma(I)$ ),  $S = 0.926$ ,  $\Delta\rho(\text{min/max}) = -0.27/0.24$  e Å<sup>-3</sup>.

**Acknowledgment.** We are grateful to the Skaggs Institute for Research and the National Institutes of Health (GM 50174) for financial support. A.S. is a Skaggs fellow. J.F. thanks DAAD (German Academic Exchange Service) for a postdoctoral fellowship. S.D. thanks the Alexander von Humboldt-Stiftung for a Feodor Lynen postdoctoral fellowship.

**Supporting Information Available:** Crystallographic data for **2a-5 MeOH**, **2d-4 EtOH**, **2a<sub>2</sub>·3a<sup>+</sup>·Cl<sup>-</sup>·7 MeOH·H<sub>2</sub>O**, **2b<sub>3</sub>·MeCN·5 H<sub>2</sub>O**, **1c·MeCN·4 H<sub>2</sub>O**, and **1d<sub>2</sub>·2 EtOH**. This material is available free of charge via the Internet at <http://pubs.acs.org>.

JO034791+

(31) Sheldrick, G. *SHELXTL*; Siemens Industrial Automation, Inc.: Madison, WI, 1993.